Polymer 51 (2010) 6203–6211

Contents lists available at ScienceDirect

Polymer

journal homepage: www.elsevier.com/locate/polymer

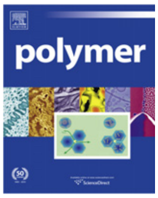

Effects of poly (vinyl alcohol) (PVA) content on preparation of novel thiol-functionalized mesoporous PVA/SiO_2 composite nanofiber membranes and their application for adsorption of heavy metal ions from aqueous solution

Shengju Wu [a], Fengting Li [a], Hongtao Wang [a], Lin Fu [a], Bingru Zhang [a,*], Guangtao Li [b]

[a] College of Environmental Science & Engineering, State Key Laboratory of Pollution Control and Resource Reuse Study, Tongji University, 1239, Siping Road, Shanghai, 200092, China
[b] Department of Chemistry, Tsinghua University, Beijing, China

ARTICLE INFO

Article history:
Received 28 May 2010
Received in revised form
22 September 2010
Accepted 10 October 2010
Available online 16 October 2010

Keywords:
Poly (vinyl alcohol)/SiO_2 composite nanofiber membranes
Electrospinning
Adsorption

ABSTRACT

Thiol-functionalized mesoporous poly (vinyl alcohol)/SiO_2 composite nanofiber membranes and pure PVA nanofiber membranes were synthesized by electrospinning. The results of Fourier transform infrared (FTIR) indicated that the PVA/SiO_2 composite nanofibers were functionalized by mercapto groups via the hydrolysis polycondensation. The surface areas of the PVA/SiO_2 composite nanofiber membranes were >290 m^2/g. The surface areas, pore diameters and pore volumes of PVA/SiO_2 composite nanofibers decreased as the PVA content increased. The adsorption capacities of the thiol-functionalized mesoporous PVA/SiO_2 composite nanofiber membranes were greater than the pure PVA nanofiber membranes. The largest adsorption capacity was 489.12 mg/g at 303 K. The mesoporous PVA/SiO_2 composite nanofiber membranes exhibited higher Cu^{2+} ion adsorption capacity than other reported nanofiber membranes. Furthermore, the adsorption capacity of the PVA/SiO_2 composite nanofiber membranes was maintained through six recycling processes. Consequently, these membranes can be promising materials for removing, and recovering, heavy metal ions in water.

1. Introduction

Heavy metal ions, often found at high concentrations in landfill leachate, pose a threat to public health [1]. In addition, many of these elements (e.g., silver, lead and copper) are precious metals, which can be recycled and reused for a wide range of applications [2]. Thus, in China and many other countries, the removal of heavy metal ions from water has attracted more and more attention from the public and government. Adsorption technology is one of the most popular methods to remove these heavy metal ions. However, adsorption efficiency, selectivity, equilibrium time, regeneration, and stability usually depend on the material characteristics of the adsorbents [3,4]. Therefore recent research has focused on the application of novel materials for adsorption of heavy metal ions from aqueous solution.

In recent years, nanoporous adsorbents have generated considerable interest due to their uniquely large specific surface area, regular pore structure, and highly controllable surface properties [4–6]. Nanoporous materials include mesoporous silica materials, mesoporous carbon materials, nanocarbon materials, nanofiber materials and others [2–6,8–11]. Mesoporous silica materials are widely used as adsorbents for adsorption of heavy metal ions, dyes and inorganic pollutants from aqueous solution in the field of water treatment [2–4]. However, most studies on mesoporous silica materials have focused on materials fabricated in bulk or in powder form [2–4]. In the field of water treatment, powdered nanoporous materials are not suitable for recycling [12,13]. Currently, researchers are focusing on ways of applying nanofiber membranes in adsorption of heavy metal ions [6,8–10,12,13].

Electrospinning is a simple, convenient, effective and widely utilized technique for generating nanofiber membrane materials, and has attracted a great deal of attention in recent years [14,15]. The electrospun fibers produced exhibit some special characteristics, such as high specific surface area, high porosity, and very small pore structures on the fibers [16–18]. It has been demonstrated that a variety of materials can be electrospun to fibers for a variety of applications, such as tissue engineering, enzyme and catalyst support, filtration media, sensors, electronic and optical devices, water treatment, drug delivery systems and reinforced nanocomposites [19–22] such as organic [23,24], inorganic [25–27], and hybrid polymers (organic-inorganic composites) [28–30]. In recent studies of chitosan nanofiber membranes [8], chloridized polyvinyl

---

* Corresponding author. Tel.: +86 21 65980567; fax: +86 21 65985059.
E-mail address: bingru@mail.tongji.edu.cn (B. Zhang).

0032-3861/$ – see front matter Crown Copyright © 2010 Published by Elsevier Ltd. All rights reserved.
doi:10.1016/j.polymer.2010.10.015

Table 1
The components of raw materials used in the synthesis of PVA/SiO_2 composites.

Components									
Gels	10 wt% PVA (g)	CTAB (g)	TEOS (g)	KH-590 (g)	Water (g)	Ethanol (g)	2 mol/L HCl (mL)	Sulfur content (wt%)	Nanofiber Membranes (PVA wt%)
G-0	0	2.19	6.64	1.54	8.64	7.37	0.8	8.37	N-0(0%)
G-1	5.0	2.19	6.64	1.54	8.64	7.37	0.8	6.43	N-1(1.43%)
G-2	7.5	2.19	6.64	1.54	8.64	7.37	0.8	6.17	N-2(2.50%)
G-3	10	2.19	6.64	1.54	8.64	7.37	0.8	6.03	N-3(3.33%)
G-4	12.5	2.19	6.64	1.54	8.64	7.37	0.8	5.79	N-4(4.00%)
G-5	15	2.19	6.64	1.54	8.64	7.37	0.8	5.57	N-5(4.55%)
G-6	5	0	0	0	0	0	0	0	N-6(100%)

chloride nanofiber membranes [6], wool keratose, silk fibroin nanofiber membranes [9], and polyacrylonitrile nanofiber membranes [10] were applied to adsorption of heavy metal ions from an aqueous solution [31,32]. However, their capacity to adsorb heavy metal ions was not high because of low surface area, low porosity, and small pore structures on the fibers. Generating polymer nanofiber membrane materials having rationally designed high porosity, high surface area, high adsorption capacity and regeneration still remains a challenge.

To increase the adsorption of heavy metals on nanofiber materials, the following methods have attracted the most attention: (1) surface modification with functional groups and (2) increasing the surface area of nanofibers [33,34]. Mesoporous nanofibers modified by functional groups have attracted much attention because of their properties such as: (1) high surface-to-volume ratio, (2) uniform pore size distribution, (3) convenient recycling, and (4) high equilibrium adsorption capacities for heavy metal ions.

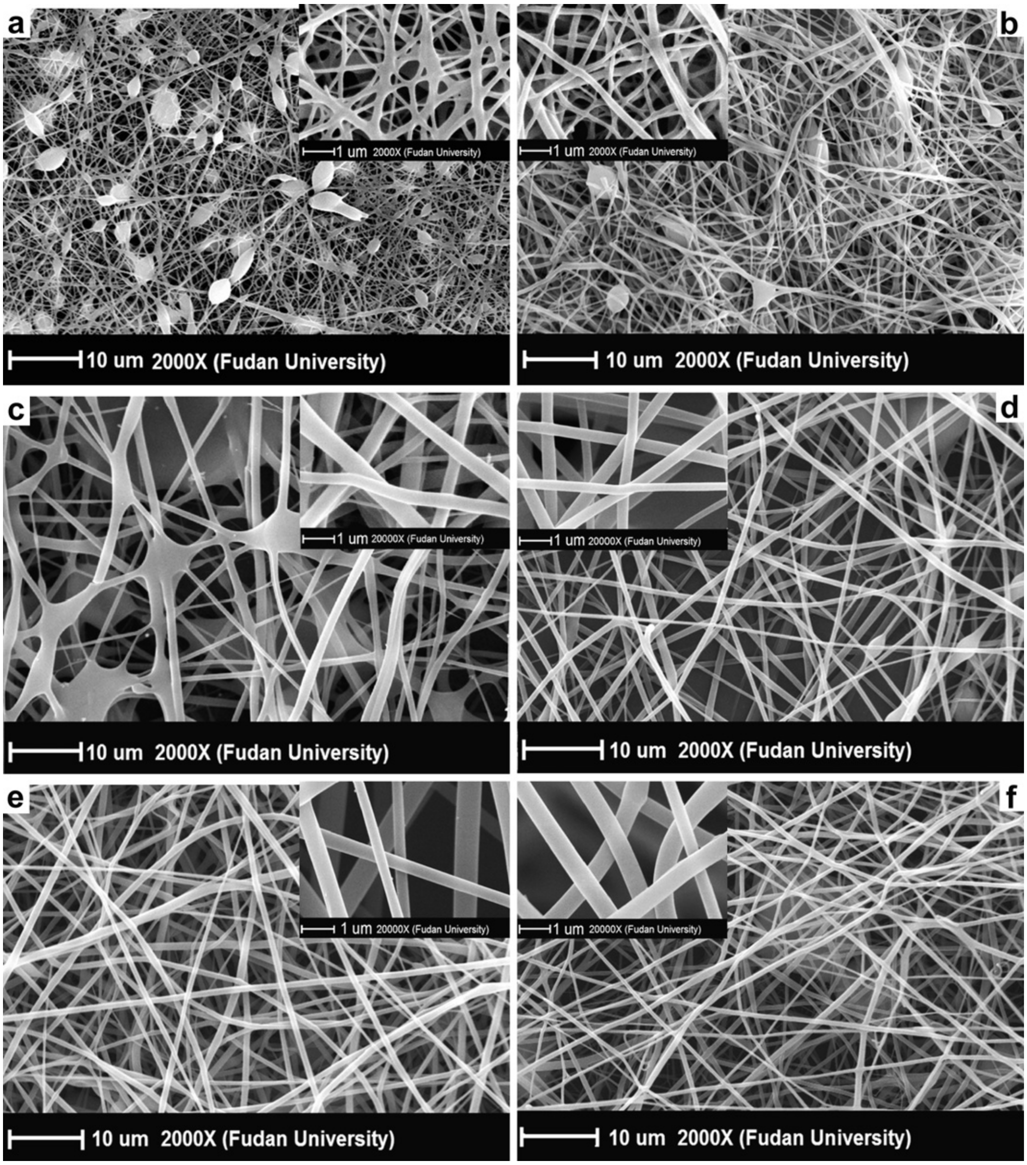

Fig. 1. SEM images of nanofibers extracted with ethanol/HCl (molar ratio of 10:1): (a) 1.43%, (b) 2.50%, (c) 3.33%, (d) 4.00%, (e) 4.55% and (f) 100%.

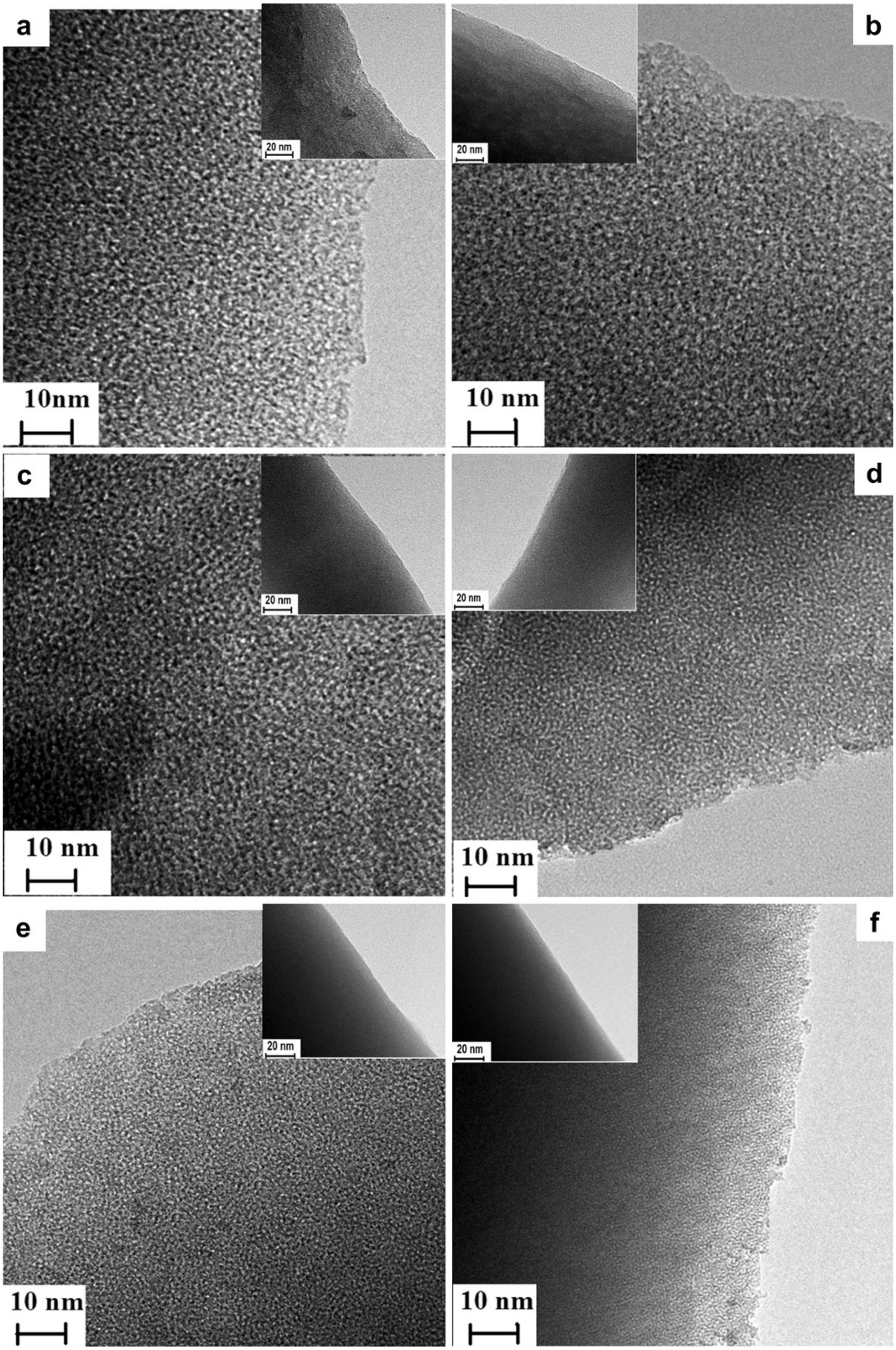

Fig. 2. TEM images of nanofibers extracted with ethanol/HCl (molar ratio of 10:1): (a) 1.43%, (b) 2.50%, (c) 3.33%, (d) 4.00%, (e) 4.55% and (f) 100%.

Mesoporous nanofiber membranes can serve as high efficiency adsorbents in adsorption of heavy metal ions and some other pollutants, such as organic molecules [3,4,31,32]. Their removal efficiency for heavy metal ions increases remarkably after the nanofiber adsorbents have been modified with $-NH_2$, $-SH$, or $-HSO_3$ functional groups, which can react with the metal ions [3,4]. For example, the sulfur atom of the $-SH$ group can form chelates with heavy metal ions [4].

PVA is known to interact with other organic [35,36] and inorganic materials [37,38]. PVA interacts with other materials upon the electrodeposition process to form a mixed membrane in a polymer matrix. The membranes are highly transparent and luminescent, with superior mechanical properties and high tenacity and intensity, and remain conducting even at high PVA content [6,8,35–39]. The PVA can supply hydroxyl groups on the surface of nanofibers. The hydroxyl groups can also serve to adsorb heavy metal ions [8]. Fiber mats of PVA/silica composite with different silica content have been successfully prepared by the electrospinning technique [40]. Mesoporous PVA/silica nanofiber membranes have been synthesized after calcination above 500 °C. However, the organic groups were removed after calcination at high temperature. The nanofiber membranes cannot be calcinated at high temperature for application in water treatment. Mesoporous PVA/SiO_2 composite nanofiber membranes have not been synthesized at room temperature until now. Polymer/silica composite nanofiber membranes functionalized with mercapto groups have distinct advantages for the specialized purposes of adsorption of heavy metal ions. Therefore, the preparation of mesoporous nanofiber membranes with high surface area, high removal efficiency for heavy metal ions and favorable recycling characteristics is a challenge for practical applications in the field of adsorption technology.

In this paper, novel mesoporous PVA/SiO_2 composite nanofiber membranes synthesized via a sol–gel electrospinning method, intended to increase the removal efficiency of heavy metal ions from waste water, are introduced. In addition, the mercapto groups on the surface of the composite nanofibers enhance their capacity to adsorb heavy metal ions. The mesoporous PVA/SiO_2 composite nanofiber membranes are suitable for applications in the field of water treatment. It is the first time that mercapto groups have been added to PVA/SiO_2 composite nanofibers to increase their removal efficiency for heavy metal ions.

2. Experiments

2.1. Reagents and materials

3-Mercaptopropyltrimethoxysilane (MPTMS, 99%) was procured from Aldrich. Tetraethyl orthosilicate (TEOS), cetyltrimethyl ammonium bromide (CTAB), absolute ethyl alcohol and poly (vinyl alcohol) (PVA, 99%, high molecular weight, MW 88000–97000) were provided by Sinopharm Chemical Reagent Company, China. Copper nitrate was used to prepare the heavy metal ion solution. Deionized (DI) water was used throughout this work.

2.2. Preparation of PVA/SiO_2 gels

A silica gel, with the molar composition TEOS:CTAB:MPTMS: HCl:H_2O:Ethanol = 1:0.31:0.188:0.025:15:5 was prepared by hydrolysis polycondensation [3,4,11]. First, 2.19 g CTAB was dissolved in 7.37 g ethanol and vigorously stirred for 0.5 h at 60 °C. Second, 8.64 g DI water and 1.54 g MPTMS were added into the mixture and further stirred for 0.5 h at 60 °C. Then, 6.64 g TEOS was slowly added into the solution mixture. Finally, 0.8 ml HCl (2 mol/L) was dropped slowly into the mixture and a silica gel was obtained after reacting for 2 h at 30 °C (G-0). 5.0 g 10 wt% PVA solution was dropped slowly into the silica gel, then the reaction proceeded in a water bath at 60 °C for another 4 h. Thus, a viscous gel of PVA/SiO_2 composite (G-1) was obtained. Four more composites with different PVA content were prepared in the same way. The PVA and sulfur contents for each of them are shown in Table 1.

2.3. Preparation of nanofiber membranes

Each of the above PVA/SiO_2 composites was placed in a plastic capillary. A copper pin connected to a high-voltage generator was placed in the solution. A grounded iron drum, covered with an aluminium foil, served as a counter electrode. A voltage of 15 kV, with a tip-to-target distance of 15 cm, at a speed of 0.3 ml/h was applied to the solution and a dense web of fibers was collected on the aluminium foil. These fibers were dried initially for 12 h at 60 °C under vacuum. Then the electrospun PVA/SiO_2 nanofiber membranes were refluxed in ethanol/HCl (molar ratio of 10:1) for 24 h at 70 °C to remove the template, and finally dried for 6 h at 60 °C under vacuum. The components of all PVA/SiO_2 nanofiber membranes (membrane N-1∼N-5) can be seen in Table 1. The sample N-6 nanofiber membrane was pure PVA nanofiber membrane and the sample N-0 nanofiber membrane was silica membrane materials.

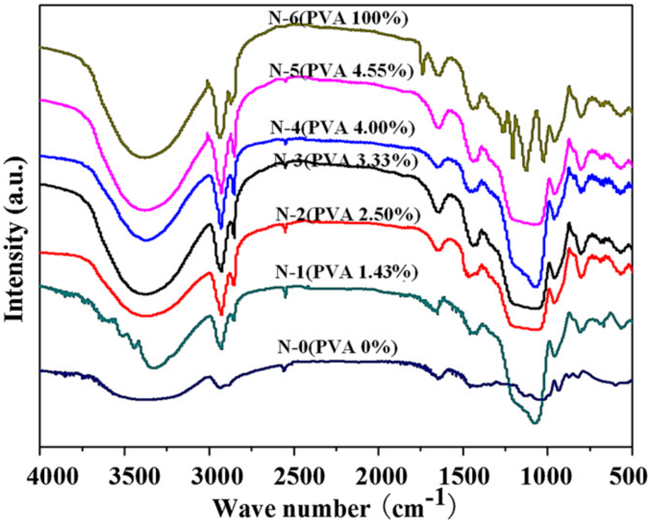

Fig. 3. FTIR spectra pattern of PVA/SiO_2 composite nanofibers extracted with ethanol/HCl (molar ratio of 10:1) at different PVA content: (N-0) 0%, (N-1) 1.43%, (N-2) 2.50%, (N-3) 3.33%, (N-4) 4.00%, (N-5) 4.55% and (N-6) 100%.

2.4. Characterization

Transmission electron microscopy (TEM) images were taken using a JEM-2011 electron microscope operating at 200 kV. Scanning electron microscopy (SEM) images were recorded with a field emission XL-30 SEM. Fourier transform infrared spectroscopy (FTIR) of KBr powder-pressed pellets was recorded on a BRUKER VECTOR 22 spectrometer. The N_2 adsorption–desorption isotherm measurements were taken with a Quantachrome NOVA 1000

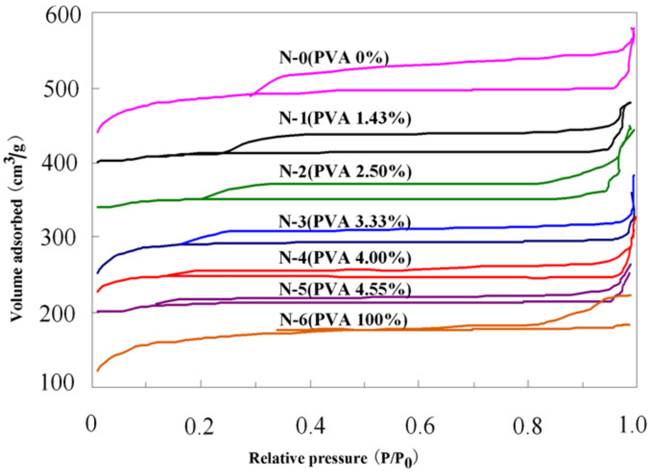

Fig. 4. The nitrogen adsorption–desorption isotherms of PVA/SiO_2 composite nanofibers extracted with ethanol/HCl (molar ratio of 10:1) at different PVA content: (N-0) 0%, (N-1) 1.43%, (N-2) 2.50%, (N-3) 3.33%, (N-4) 4.00%, (N-5) 4.55% and (N-6) 100%.

Table 2
Physical properties of nanofiber membranes.

Sample	PVA conten (wt%)	Surface area (m^2/g)	Pore diameter (nm)	Pore volume (cm^3/g)	Nanofiber diameter (nm)
N-0	0	521.7	6.72	0.657	500–1000
N-1	1.43	474.3	4.72	0.457	100–300
N-2	2.50	431.5	4.13	0.421	200–400
N-3	3.33	370.2	3.83	0.357	300–500
N-4	4.00	347.9	3.41	0.313	400–600
N-5	4.55	294.7	2.85	0.274	500–700
N-6	100	34.7	0.13	0.034	600–1000

system. Wide-angle x-ray diffraction (WARD) patterns of the samples were recorded using a Philips diffractometer with a Geiger counter. Scans were made from 10° to 90° (2θ) at the speed of 2 °/min. The concentrations of Cu^{2+} remaining in the solutions were analyzed by an Inductively Coupled Plasma Spectrometer (ICP, Optima 2100 DV, America). The sulfur content was determined by an Elemental Analyser (Vario EL,CHNS).

2.5. Effect of pH on adsorption

The effect of pH on the adsorption was determined in experiments using approximately 50 mg of membrane and 100 ml of 1.0 mmol/L Cu^{2+} solution. Dilute nitric acid and sodium hydroxide solutions were used to adjust the initial pH value to 2, 2.5, 3, 3.3, 3.7, 4, 4.5, 5, 5.5 and 6. After shaking (200 r/min) for 60 min at 303 K, the suspension was separated with a 0.45 μm Uniflo filter. The filtrate was analyzed for Cu^{2+} by ICP/OES spectroscopy and the final pH value of the filtrate was determined.

2.6. The adsorption isotherm on the nanofiber membranes

Adsorption experiments were conducted as follows. For each 250 ml conical flask, approximately 50 mg of membranes and 100 ml of Cu^{2+} solution, each with different concentrations (0.5, 1.0, 1.5, 2.0, 3.0, 4.0, 5.0, 7.0 and 10.0 mmol/L, respectively) were added. Dilute nitric acid and sodium hydroxide solutions were used to adjust the initial pH value to 5. The oscillation treatment consisted of oscillations at 200 r/min at temperature of 303 K for 60 min. Then, the suspension was separated using a 0.45 μm Uniflo filter. The filtrate was determined for Cu^{2+} concentration by using ICP/OES spectroscopy.

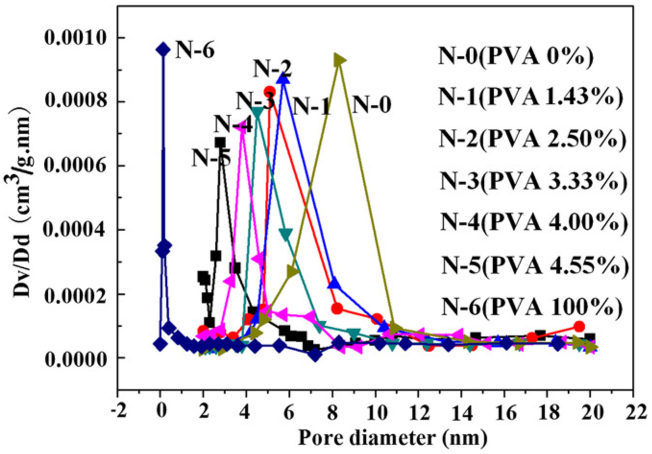

Fig. 5. The pore size distributions of PVA/SiO_2 composite nanofibers extracted with ethanol/HCl (molar ratio of 10:1) at different PVA content: (N-0) 0%, (N-1) 1.43%, (N-2) 2.50%, (N-3) 3.33%, (N-4) 4.00%, (N-5) 4.55% and (N-6) 100%.

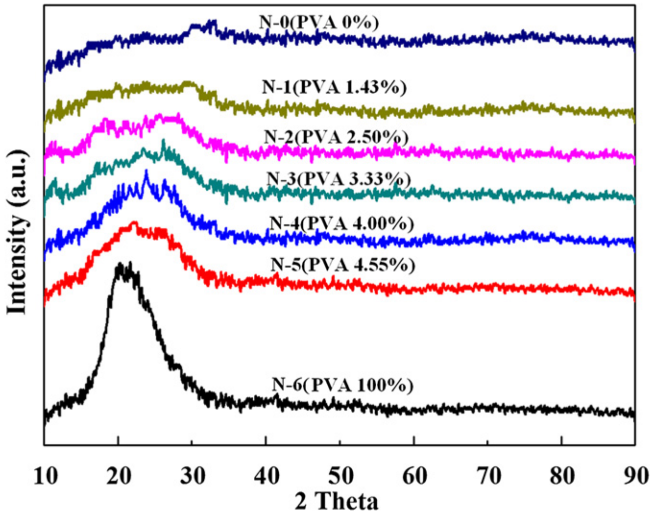

Fig. 6. WARD of PVA/SiO_2 composite nanofibers extracted with ethanol/HCl (molar ratio of 10:1) at different PVA content: (N-0) 0%, (N-1) 1.43%, (N-2) 2.50%, (N-3) 3.33%, (N-4) 4.00%, (N-5) 4.55% and (N-6) 100%.

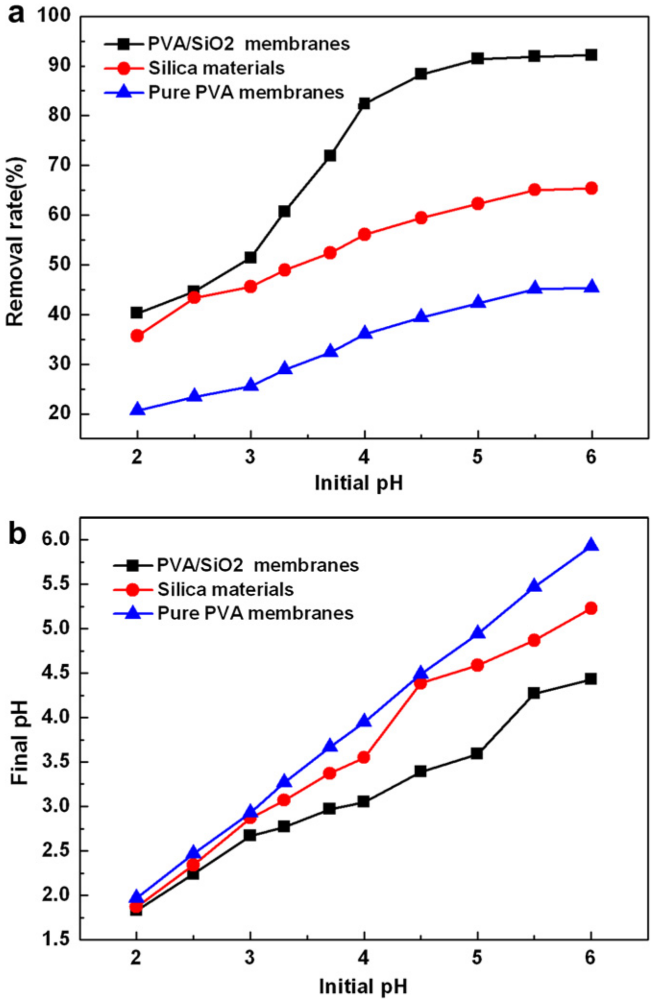

Fig. 7. Effects of pH on adsorption for PVA/SiO_2 composite nanofibers, silica materials, pure PVA nanofibers and changes of the final and initial pH values.

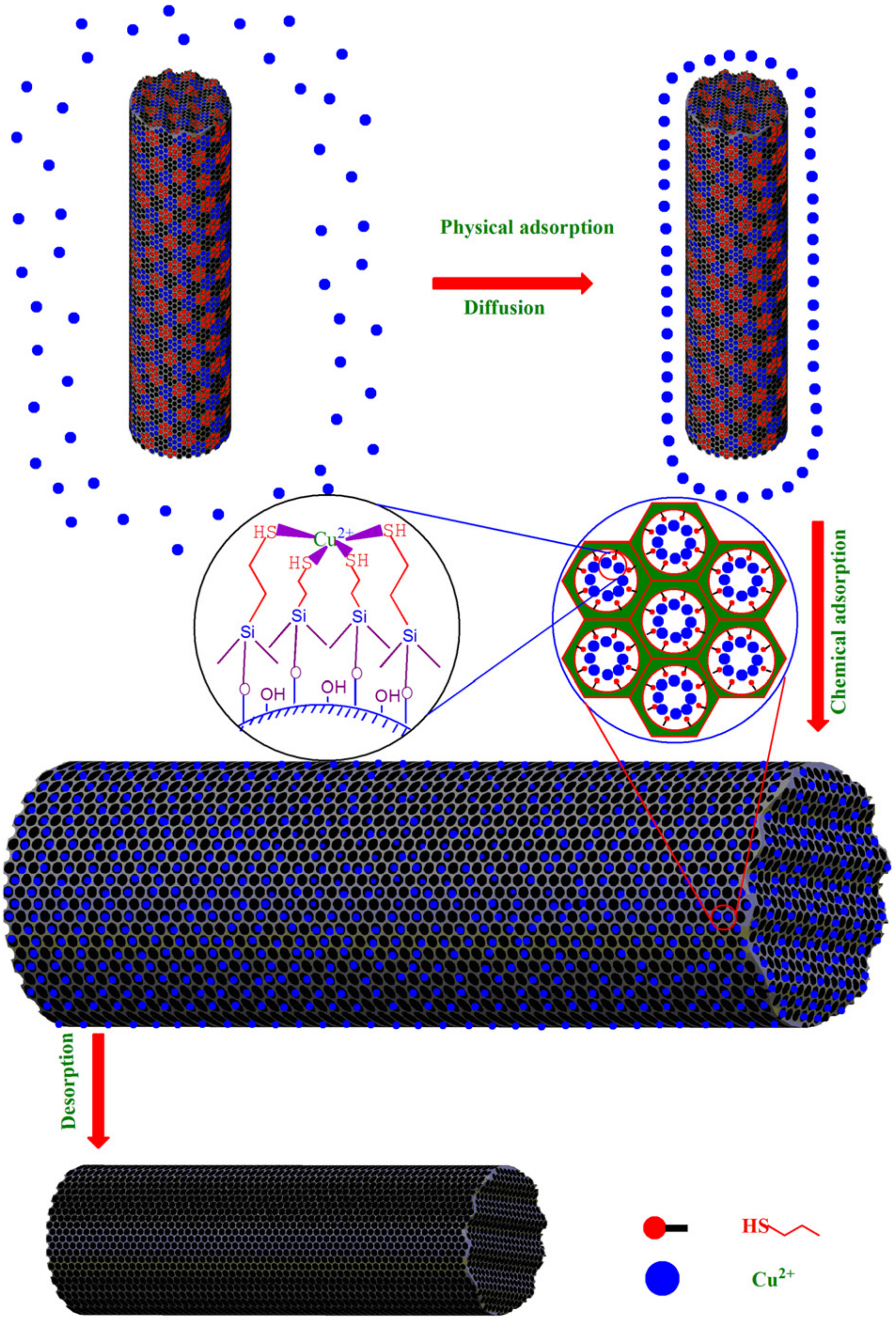

Fig. 8. The mechanism of adsorption of Cu^{2+} on PVA/SiO_2 composite nanofibers.

2.7. *Regeneration of nanofiber membranes*

About 100 ml of 1.0 mmol/L Cu^{2+} solution was added to a 250 ml conical flask containing 50 mg of nanofiber membranes. After an oscillation treatment for 60 min at a temperature of 303 K, the suspension was separated using a 0.45 μm Uniflo filter. The filtrate was determined for Cu^{2+} concentration by using ICP/OES spectroscopy. The copper-loaded adsorbent was then stirred in 100 ml of 1 mol/L HCl solution for 2 h at room temperature to strip the Cu^{2+} ion. Then the suspension was filtered and the residue was added to 1 mol/L $NaHCO_3$ solution with a stirring time of 2 h at room temperature. After filtration and washing, the sample was neutralized to pH 7. The cleaned membrane was then dried in a vacuum oven at 60 °C. The first adsorption–desorption cycle was followed by five other cycles using the same adsorbent batch. After six regeneration cycles, the sample was dissolved using 100 ml dilute nitric acid for 3 h. The solution was then diluted to 500 ml to measure the Cu^{2+} ion concentration using ICP/OES spectroscopy.

3. Results and discussions

3.1. *Characterization of nanofiber membranes*

Fig. 1 shows SEM photographs of nanofibers spun at a voltage of 15 kV, with a tip-to-target distance of 15 cm, and extracted with ethanol/HCl (molar ratio of 10:1).

As observed, the diameters of PVA/SiO$_2$ composite nanofibers were in the range of 100–700 nm, and the diameters of pure PVA nanofibers ranged from 600 to 1000 nm. The diameters of PVA/SiO$_2$ composite nanofibers were less than those of pure PVA nanofibers. When the amount of PVA decreased, the diameters of the nanofibers also decreased. However, there were some bears in the membrane when the content of PVA was less than 3.33%. When the PVA content was greater than 3.33%, the amount of bears decreased and the nanofiber diameters were more uniform. However, there were more crosslinks between the fibers [40–45].

Fig. 2 shows TEM photographs of thiol-functionalized mesoporous PVA/SiO$_2$ composite nanofibers. The TEM images confirmed that the nanofibers obtained after extraction with ethanol/HCl had both porous and rough surfaces. The surfaces of the nanofibers were mesostructured. Although the body-centered mesostructure was out-of-order, the large specific surface area, high porosity, small pore structures, and highly controllable surface properties ensure that PVA/SiO$_2$ composite nanofibers can serve as an adsorbent with large adsorption capacity [3,4].

Fig. 3 shows the FTIR spectra for the silica materials, pure PVA nanofibers and PVA/SiO$_2$ composite nanofibers extracted with ethanol/HCl for 24 h. For the PVA spectrum, the broad band observed from 3100 to 3600 cm^{-1} was assigned to –OH stretching due to the strong hydrogen bonding of intramolecular and intermolecular type. The stretching band at 285–2950 cm^{-1} was attributed to the alkyl stretching mode. The absorption band from 1700 to 1750 cm^{-1} arises due to the stretching vibration of the carbonyl from the acetage group present in the partially hydrolyzed PVA polymer [46]. For silica materials spectrum, the features around 801 and 1053 cm^{-1} are assigned to the Si–O–Si stretching vibrations. The vibrations of Si–OH appeared around 1653 and 3404 cm^{-1} [3,4,11]. The FTIR spectra in Fig. 3 show characteristic bands for mercapto group vibrations around 2552 cm^{-1} [4,41,47], which leads to the conclusion that mercapto groups have been successfully added to the mesoporous silica skeleton by hydrolysis polycondensation.

The nitrogen adsorption–desorption isotherms for PVA/SiO$_2$ composite nanofibers extracted are shown in Fig. 4, respectively. Based on BJH theory, the average pore diameter, the Brunauer-Emmet-Teller (BET) surface area and the pore volume of fibers extracted are shown in Table 2. It indicates that the surface area, pore volume and pore diameter decreased as the PVA content increased.

The pore size distributions of PVA/SiO$_2$ composite nanofiber membranes are shown in Fig. 5. As shown in Fig. 5, the diameters of PVA/SiO$_2$ composite nanofibers were in the range of 2.85–4.72 nm, indicating that the nanofiber surface was mesoporous. The pore diameter of pure PVA nanofibers is on 0.13 nm.

Fig. 6 shows the WARD curve for the nanofiber samples. As shown in Fig. 6 one peak appeared at around $2\theta = 20°$, corresponding to the (101) plane of semi-crystalline PVA in pure PVA nanofibers. However, the peak broadened for the samples of PVA/SiO$_2$ composite nanofibers, indicating that the crystallinity of PVA was substantially influenced by the presence of silica in the PVA/SiO$_2$ composite nanofibers.

3.2. Effect of pH on adsorption

The effects of the solution pH on the adsorption of Cu^{2+} onto nanofiber membranes are shown in Fig. 7. The Cu^{2+} removal efficiency increased remarkably as the solution pH increased from 2 to 5, then increased slowly with further increases in pH. This effect was mainly due to the protonation of the sulfur atom of the –SH group, which diminishes the ability of the –SH group to be involved in chelating Cu^{2+} from solution. When the pH was around 5, the heavy metals in solution existed in the form Cu(OH)$^+$, which favors adsorption [3,4,6–8]. The removal rate of PVA/SiO$_2$ composite nanofibers is highest, and the pure PVA nanofibers is lowest.

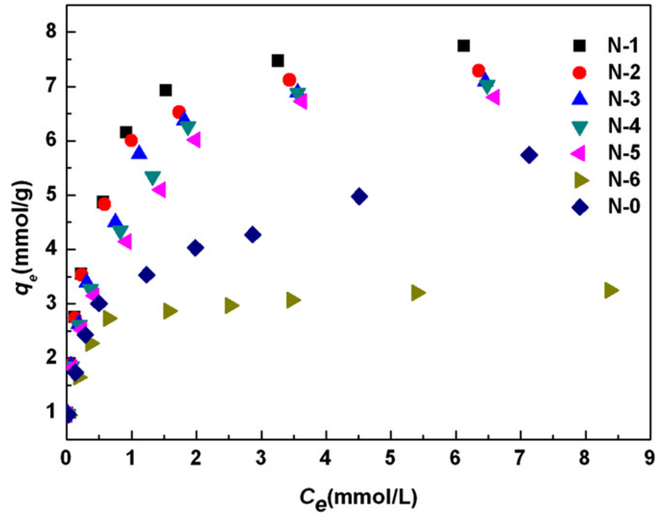

Fig. 9. Adsorption isotherm of PVA/SiO$_2$ composite nanofiber membranes, silica materials and pure PVA nanofiber membranes. (N-0) 0%, (N-1) 1.43%, (N-2) 2.50%, (N-3) 3.33%, (N-4) 4.00%, (N-5) 4.55% and (N-6) 100%.

As shown in Fig. 7(b), when the adsorption process was complete the final solution pH was lower than the initial pH value. An exchange adsorption reaction between H$^+$ of the –SH group in the framework of mesoporous materials and the heavy metal ions caused a general decline in the pH of the system. Fig. 8 shows the adsorption mechanism of Cu^{2+} onto the adsorbent [2,4,48,49]. The mechanism for the removal of toxic heavy metal ions in an aqueous solution is mostly either by electrostatic interaction (ionic interaction between positively charged metal ions and negatively charged matrices) or by chelation (donation of the lone-pair electrons of the matrices to metal ions to form co-ordinate bonds) [48,49]. The final pH of PVA/SiO$_2$ composite nanofibers is lowest, and the pure PVA nanofibers is highest.

The optimum pH value for the removal of Cu^{2+} from solution ranged from 5 to 6. In this pH range, neither precipitation of the metal hydroxide nor protonation of the sulfur atom on the –SH group occurred.

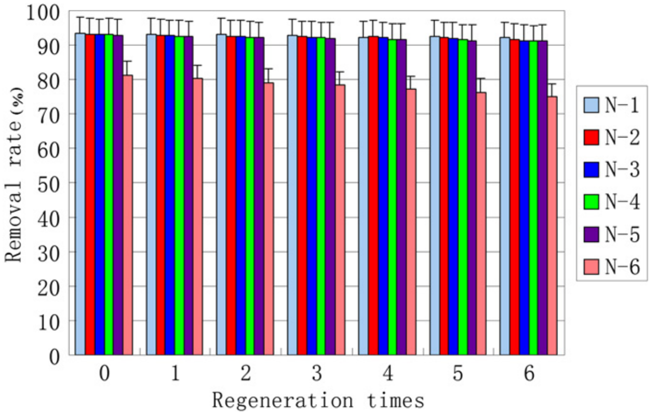

Fig. 10. Removal efficiency of Cu^{2+} on nanofiber membranes at different regeneration cycles. (N-1) 1.43%, (N-2) 2.50%, (N-3) 3.33%, (N-4) 4.00%, (N-5) 4.55% and (N-6) 100%.

Table 3
Non-linear fitting parameters, equations of the Redlich–Peterson model.

Membranes (PVA wt%)	Adsorption capacity (mg/g)	Average value of fitting parameter				Equation
		P	α	β	R^2	
N-0(0%)	389.12	59.24	16.23	1.001	0.9987	$q_e = 59.24C_e/(1+16.23C_e^{1.001})$
N-1(1.43%)	489.12	62.67	18.09	1.003	0.9994	$q_e = 62.67C_e/(1+18.09C_e^{1.003})$
N-2(2.50%)	423.87	60.17	17.02	0.9790	0.9986	$q_e = 60.17C_e/(1+17.02C_e^{0.9790})$
N-3(3.33%)	373. 37	59.01	15.81	0.9455	0.9991	$q_e = 59.01C_e/(1+15.81C_e^{0.9455})$
N-4(4.00%)	389.12	56.18	13.12	0.9691	0.9979	$q_e = 56.18C_e/(1+13.12C_e^{0.9691})$
N-5(4.55%)	341.43	52.67	13.09	1.003	0.9994	$q_e = 52.67C_e/(1+13.09C_e^{1.003})$
N-6(100%)	124.34	16.47	5.80	1.009	0.9988	$q_e = 16.47C_e/(1+5.80C_e^{1.009})$

3.3. Adsorption isotherm of PVA/SiO$_2$ composite nanofibers

Redlich–Peterson equations (Eq. (1)) were used to analyze the experimental adsorption isotherms in Fig. 5.

$$q_e = \frac{PC_e}{1+\alpha C_e^{\beta}} \tag{1}$$

In the above equation, q_e is the sorption amount per unit of adsorbent (mmol/g), C_e is the equilibrium concentration (mmol/L) of heavy metal ions, P is the Redlich–Peterson isotherm constant (l/mmol), α is the Redlich–Peterson isotherm constant (l/mmol), and β is the exponent, which lies between 0 and 1.

The isotherms of Redlich–Peterson models for Cu^{2+} adsorption on PVA/SiO$_2$ composite nanofibers are displayed in Fig. 9, and the corresponding parameters are listed in Table 3. The adsorption of Cu^{2+} ions increased rapidly in the initial phase and then the increasing trend decreased as the initial concentration increased. The initial increase might be due to the high surface area, many available binding sites (such as mercapto groups, primary and secondary hydroxyl groups), and inter and intra pores in the adsorbent [2–4]. The adsorption equilibrium data of Cu(II) ions was analyzed with the Redlich–Peterson adsorption equation. The adsorption data fit the Redlich–Peterson isotherm equation well. The β constant of the Redlich–Peterson isotherm equation was nearly equal to 1 [2,49], which indicates that the monolayer reaction of Cu^{2+} on PVA/SiO$_2$ composite nanofibers was predominant, but it was not an ideal monolayer adsorption. The main adsorption process of the mesoporous adsorbents for heavy metal ions is chemisorption.

From Fig. 9, it is clear that the adsorption capacities of the PVA/SiO$_2$ composite nanofiber membranes were $>=$ 341.43 mg/g at 303 K, and the largest equilibrium adsorption capacity of Cu^{2+} was 489.12 mg/g on PVA/SiO$_2$ composite nanofiber membrane (membrane N-1). The result is higher than other results reported in other research. The equilibrium adsorption capacities of copper ions by chitosan nanofiber membranes, chloridized polyvinyl chloride nanofiber membranes, wool keratose, silk fibroin nanofiber membranes, polyacrylonitrile nanofiber membranes, and mesoporous silica materials were 485.44 mg/g, 100.83 mg/g, 2.88 mg/g, 27.95 mg/g, 12.82 mg/g, and 36.38 mg/g, respectively [3,4,6–10]. However, when the initial concentration of heavy metal ions is too high, there may be a coprecipitation reaction between heavy metal ions [32,49]. The remarkable characteristics of the thiol-functionalized mesoporous silica materials are the high surface area per unit mass and large number of mercapto groups, which may cause high adsorption capacity for metal ions.

Table 3 shows the equilibrium adsorption capacity of Cu^{2+} on PVA/SiO$_2$ composite nanofibers and pure PVA nanofibers. It is clear that the equilibrium adsorption capacity of heavy metal ions on functionalized mesoporous PVA/SiO$_2$ composite nanofiber membranes was larger than on pure PVA nanofiber membranes. Thus, functionalizing the nanofiber membranes with mercapto groups was an effective way to improve the equilibrium adsorption capacity of heavy metal ions on the adsorbent.

3.4. Regeneration for nanofiber membranes

The stripping agent used in this experiment was 1 mol/L HCl solution. As shown in Fig. 10, for PVA/SiO$_2$ composite nanofiber membranes, the adsorption efficiency of Cu^{2+} decreased only from 93.1 to 90.13 even in six extraction cycles. The adsorption efficiency of Cu^{2+} decreased from 83.7 to 76.21 for pure PVA membranes. It indicates that the adsorption capacity of PVA/SiO$_2$ composite nanofiber membranes for Cu^{2+} ion was almost fully restored. The regeneration of PVA/SiO$_2$ composite nanofiber membranes is better than that of pure PVA nanofiber membrane. Consequently PVA/SiO$_2$ composite nanofiber membranes can be promising materials for removing, and recovering, heavy metal ions in water.

4. Conclusions

In summary, we demonstrated a novel approach to preparation of PVA/SiO$_2$ composite nanofiber membranes with mesostructure functionalized with mercapto groups without calcination. Electrospun nanofiber membranes, which have large surface areas per unit volume, mass, and number of mercapto groups, can very suitably remove specific materials by adsorption based on chemical or physical affinity. When the PVA content of PVA/SiO$_2$ composite nanofiber membranes was in the range of 1.43–4.55%, the surface areas of PVA/SiO$_2$ composite nanofiber membranes were $>$290 m^2/g. The surface area, pore diameter and pore volume decreased when the PVA content increased. The mesoporous PVA/SiO$_2$ composite nanofiber membranes exhibited higher Cu^{2+} ion adsorption capacity than other reported nanofiber membranes. The largest was 489.12 mg/g. Furthermore, the adsorption capacity of PVA/SiO$_2$ composite nanofiber membranes was maintained through six recycling processes of adsorption and desorption. The adsorption capacities of thiol-functionalized mesoporous PVA/SiO$_2$ composite nanofiber membranes were greater than those of pure PVA nanofiber membrane. It is seen that surface modification is a useful tool for improving the performance of an adsorbent. Consequently, this membrane can be a promising material for removing, and recovering, heavy metal ions in water.

Acknowledgements

The work was supported by the State Key Special Funds for Water Program (Project Number 2008ZX07421-002), as well as the China-American Cooperation for 10 + 10 program (2009DFA90740), and the Ministry of Science and Technology. The Science & Technology Commission, in Shanghai, also sponsored this research.

References

[1] Zhang QR, Pan BC, Pan BJ, Zhang WM, Jia K, Zhang QX. Environ Sci Technol 2008;42:4140.
[2] Mureseanu M, Reiss A, Stefanescu I, David E, Parvulescu V, Renard G, et al. Chemosphere 2008;73:1499.
[3] Yang H, Xu R, Xue XM, Li FT, Li GT. J Hazard Mater 2008;152:690.
[4] Xue XM, Li FT. Microporous Mesoporous Mater 2008;116:116.
[5] Shevchenko N, Zaitsev V, Walcarius A. Environ Sci Technol 2008;42:6922.
[6] Sang YM, Li FS, Gu QB, Liang CZ, Chen JQ. Desalination 2008;223:349.
[7] Castricum HL, Sah A, Mittelmeijer-Hazeleger MC, Elshof JE. Microporous Mesoporous Mater 2005;83:1.
[8] Haider S, Park SY. J Memb Sci 2009;328:90.
[9] Ki CS, Gang EH, Um IC, Park YH. J Memb Sci 2007;302:20.
[10] Deng SB, Bai RB, Chen JP. J Colloid Interface Sci 2003;260:265.
[11] Wu SJ, Li FT, Xu R, Wei SH, Li GT. J Nanopart Res 2010;12:2111.
[12] Barakat NAM, Kim BS, Kim HY. J Phys Chem C 2009;113:531.
[13] Zhang LF, Hsieh YL. Nanotechnology 2006;17:4416.
[14] Dzenis Y. Science 2004;304:1917.
[15] Zhang DM, Chang J. Nano Lett 2008;8:3283.
[16] Mccann JT, Marquez M, Xia YN. J Am Chem Soc 2006;128:1436.
[17] Liu Y, Pellerin C. Macromolecules 2006;39:8886.
[18] Wang LL, Hou ZY, Quan ZW, Li CX, Yang J, Lian HZ, et al. Inorg Chem 2009;48:6731.
[19] Wu H, Sun Y, Lin DD, Zhang R, Zhang C, Pan W. Adv Mater 2009;21:227.
[20] Yang DY, Niu X, Liu YY, Wang Y, Gu X, Song LS, et al. Adv Mater 2008;20:4770.
[21] Yang DJ, Zheng ZF, Zhu HY, Liu HW, Gao XP. Adv Mater 2008;20:2777.
[22] Agarwal S, Greiner A, Wendorff JH. Adv Funct Mater 2009;19:1.
[23] Torres-Giner S, Gimeno-Alcaniz JV, Ocio MJ, Lagaron JM. ACS Appl Mater Interfaces 2009;4:218.
[24] Bazilevsky AV, Yarin AL, Megaridis CM. Langmuir 2007;23:2311.
[25] Dai YQ, Cobley CM, Zeng J, Sun YM, Xia YN. Nano Lett 2009;9:2455.
[26] Shui JL, Li JC. Nano Lett 2009;9:1307.
[27] Formo E, Lee E, Campbell D, Xia YN. Nano Lett 2008;8:668.
[28] Nikiforov M, Liu HQ, Craighead H, Bonnell D. Nano Lett 2006;6:896.
[29] Patel AC, Li SX, Yuan JM, Wei Y. Nano Lett 2006;6:1042.
[30] Kim C, Nhu-Ngoc BT, Yang KS, Kojima M, Kim YA, Kim YJ, et al. Adv Mater 2007;19:2341.
[31] Saeed K, Haider S, Oh TJ, Park SY. J Memb Sci 2008;322:400.
[32] Deitzel JM, Kosik W, Mcknight SH, Beck NC, Desimone JM, Crette S. Polymer 2002;43:1025.
[33] Qiu YJ, Yu J, Rafique J, Yin J, Bai XD, Wang EG. J Phys Chem C 2009;113:11228.
[34] Ostermann R, Li D, Yin YD, McCann JT, Xia YN. Nano Lett 2006;6:1297.
[35] Demir MM, Özen B, Özcelik S. J Phys Chem B 2009;113:11568.
[36] Stoiljkovic A, Venkatesh R, Klimov E, Raman V, Wendorff JH, Greiner A. Macromolecules 2009;42:6147.
[37] Wu H, Zhang R, Liu XX, Lin DD, Pan W. Chem Mater 2007;19:3506.
[38] Pauporté T. Cryst Growth Des 2007;7:2310.
[39] Peng Q, Sun XY, Spagnola JC, Saquing C, Khan SA, Spontak RJ, et al. ACS Nano 2009;3:546.
[40] Shao CL, Kim HY, Gong J, Ding B, Lee DR, Park SJ. Mater Lett 2003;57:1579.
[41] Rambaud F, Vallé K, Thibaud S, Julián-López B, Sanchez C. Adv Funct Mater 2009;19:1.
[42] Yu W, Lan CH, Wang SJ, Fang PF, Sun YM. Polymer 2010;51:2403.
[43] Zhang D, Karki AB, Rutman D, Young DP, Wang A, Cocke D, et al. Polymer 2009;50:4189.
[44] Kriegel C, Kit KM, McClements DJ, Weiss J. Polymer 2009;50:189.
[45] Agarwal S, Wendorff JH, Greiner A. Polymer 2008;49:5603.
[46] Jeun JP, Jeon YK, Nho YC, Kang PH. J Ind Eng Chem 2009;15:430.
[47] Keyur D, Kit K, Li JJ, Zivanovic S. Biomacromolecules 2008;9:1000.
[48] Cestari AR, Vieira EFS, Vieira GS, Costa LP, Tavares AMG, Loh W, et al. J Hazard Mater 2009;161:307.
[49] Quintelas C, Rocha Z, Silva B, Fonseca B, Figueiredo H, Tavares T. Chem Eng J 2009;149:319.